Article:
Hadianamrei, R., Anas Tomeh, M., Brown, S. orcid.org/0000-0002-7581-7491 et al. (2 more authors) (2022) Rationally designed short cationic α-helical peptides with selective anticancer activity. Journal of Colloid and Interface Science, 607 (Part 1). pp. 488-501. ISSN 0021-9797

https://doi.org/10.1016/j.jcis.2021.08.200

Journal of Colloid and Interface Science 607 (2022) 488–501

Contents lists available at ScienceDirect

Journal of Colloid and Interface Science

journal homepage: www.elsevier.com/locate/jcis

Rationally designed short cationic α-helical peptides with selective anticancer activity

Roja Hadianamrei [a], Mhd Anas Tomeh [a], Stephen Brown [c], Jiqian Wang [d], Xiubo Zhao [a,b,*]

[a] Department of Chemical and Biological Engineering, University of Sheffield, S1 3JD, UK
[b] School of Pharmacy, Changzhou University, Changzhou 213164, China
[c] Department of Biomedical Science, University of Sheffield, S10 2TN, UK
[d] Centre for Bioengineering and Biotechnology, China University of Petroleum (East China), Qingdao 266555, China

GRAPHICAL ABSTRACT

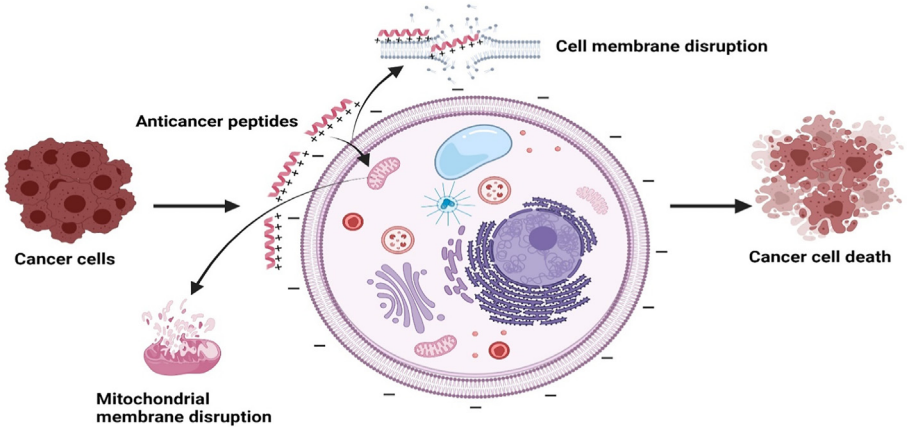

ARTICLE INFO

Article history:
Received 15 June 2021
Revised 8 August 2021
Accepted 30 August 2021
Available online 1 September 2021

Keywords:
Anticancer peptides
Cationic amphiphilic peptides
Helical peptides
Membrane penetration
Cancer cell targeting

ABSTRACT

Hypothesis: Naturally derived or synthetic anticancer peptides (ACPs) have emerged as a new generation of anticancer agents with higher selectivity for cancer cells and less propensity for drug resistance. Despite the structural diversity of ACPs, α-helix is the most common secondary structure among them. Herein we report the development of a new library of short cationic amphiphilic α-helical ACPs with selective cytotoxicity against colorectal and cervical cancer.

Experiments: The peptides had a general formula $C(XXYY)_3$ with C representing amino acid cysteine (providing a -SH group for molecular conjugation), X representing hydrophobic amino acids (isoleucine (I) or leucine (L)), and Y representing cationic amino acids (arginine (R) or lysine (K)). Two variants of the peptides were synthesized by adding additional Isoleucine residues to the C-terminal and replacing the *N*-terminal cysteine with LC-propargylglycine (LC-G) to investigate the effect of *N*-terminal and C-terminal variation on the anticancer activity. The structure and physicochemical properties of the peptides were determined by RP-HPLC, LC-MS and CD spectroscopy. The cytotoxicity of the peptides in different cell lines was assessed by MTT test, cell proliferation assay and mitochondrial damage assay. The mechanism of cell selectivity of the peptides was investigated by studying their interfacial behaviour at the air/water and lipid/water interface using Langmuir trough.

* Corresponding author at: Department of Chemical and Biological Engineering, University of Sheffield, S1 3JD, UK
E-mail address: xiubo.zhao@sheffield.ac.uk (X. Zhao).

https://doi.org/10.1016/j.jcis.2021.08.200
0021-9797/

Findings: The peptides consisting of K residues in their hydrophilic domains exhibited more selective anticancer activity whereas the peptides containing R exhibited strong toxicity in normal cells. The anticancer activity of the peptides was a function of their helical content and their hydrophobicity. Therefore, the addition of two I residues at C-terminal enhanced the anticancer activity of the peptides by increasing their hydrophobicity and their helical content. These two variants also exhibited strong anticancer activity against colorectal cancer multicellular tumour spheroids (MCTS). The higher toxicity of the peptides in cancer cells compared to normal cells was the result of higher penetration into the negatively charged cancer cell membranes, leading to higher cellular uptake, and their cytotoxic effect was mainly exerted by damaging the mitochondrial membranes leading to apoptosis. The results from this study provide a basis for rational design of new α-helical ACPs with enhanced anticancer activity and selectivity.

1. Introduction

Cancer is the second leading cause of death in the world and is generally caused by "driver mutations" in the genes which are involved in key cellular functions which enable the cancer cells to evade growth suppression, resist cell death, and activate invasion and metastasis [1–4]. The current cancer treatment strategies mainly include chemotherapy, radiotherapy, surgery, and immunotherapy. These treatment strategies often lack selectivity for cancer cells which leads to adverse effects that significantly reduce the quality of life of the patients and can lead to discontinuation of therapy [5–17,3,18–27] or may even induce life threatening hypersensitivity reactions [16,27,28]. Another major concern with many of the currently available anticancer agents is development of drug resistance which can lead to cancer relapse [5,29]. Hence, there is still an ongoing quest for development of alternative cost-effective anticancer therapies with selective toxicity to cancer cells without causing damage to the normal healthy tissues, and with lower propensity for resistance.

Recently, anticancer peptides (ACPs) have emerged as a new alternative to conventional anticancer drugs. Naturally occurring antimicrobial peptides (AMPs) or host defence peptides are an essential component of the innate immunity against pathogens in different organisms such as plants, insects, amphibians, and mammals [30–34]. More recently, it has been evidenced that some AMPs also possess selective anticancer activity suggesting them as promising anticancer drugs [34–36]. The smaller size and higher solubility of the ACPs compared to monoclonal antibodies provides better pharmacokinetics, higher cellular uptake in the target tissue and rapid clearance from the non-target tissues which is favourable for anticancer agents [35]. Despite the structural diversity among ACPs, they all share some common structural features such as short sequence (5–50 amino acid residues), positive charge and amphiphilic nature which are essential to their biological activity [30–34].

The higher selectivity of the ACPs for cancer cells over normal cells is supposed to be attributed to the higher affinity of the cationic peptides for the anionic membrane of the cancer cells compared to the zwitterionic membrane of the normal mammalian cells [30–34,36,37]. The presence of anionic phospholipids such as phosphatidylserine (PS) and higher expression of anionic molecules such as heparan sulfates and O-glycosylated mucins in the outer leaflet of the cancer cell membranes renders them more negatively charged than the membrane of the normal cells which are mainly composed of zwitterionic lipids such as phosphatidylcholine (PC) and sphingomyelin [30–34,36,37]. This targeting mechanism is not affected by the tumour heterogeneity and is less prone to drug resistance which is a great advantage over the other classes of anticancer drugs [31,33,34]. Over the last decade, various types of naturally occurring or synthetic anticancer peptides have been introduced as efficient anticancer therapies some of which have found their way to clinical trials [31,38]. The high production costs, poor bioavailability due to enzymatic proteolysis, and risk of immunogenicity with naturally occurring ACPs has shifted the ACP research towards the development of synthetic ACPs with enhanced efficacy and improved physicochemical properties [31,33,39–43]. The design strategies mainly include template modification, minimalist de novo design, combinatorial library technology and in silico models [40,42,44–53].

Herein, we report the development of a new series of synthetic α-helical anticancer peptides with selective anticancer activity towards colorectal and cervical cancer cells and minimal toxicity in human dermal fibroblasts. The peptides were designed using minimalist de novo design strategy based on the basic structural features required for α-helical ACPs. The cytotoxicity of the designed anticancer peptides in normal and cancer cells was studied and compared. Furthermore, the surface activity of the designed ACPs at the air/water interface and their interaction with different types of lipid mono and bilayers as models of normal and cancer cell membranes were studied to provide an insight into the structure activity relationship of this group of peptides.

The general formula for this series of anticancer peptides is C $(XXYY)_3$, with C representing amino acid cysteine, X representing hydrophobic amino acids (isoleucine (I) or leucine (L)), and Y representing cationic amino acids (arginine (R) or lysine (K)). This combination of hydrophobic and cationic amino acids in the repeat unit was expected to confer α-helical conformation on the peptide upon contact with amphiphilic membranes and the *N*-terminal cysteine was added to improve the helical propensity [43,49]. Moreover, the cysteine residue provides a site for conjugation of the peptide to other molecules via the -SH group. Two variants of these peptides were designed by adding additional isoleucine residues to the C-terminal to further stabilize the peptide molecule and to increase its hydrophobicity [43]. In one of the variants, the *N*-terminal cysteine was replaced with LC-propargylglycine (LC-G) to investigate the effect of *N*-terminal variation on the stability of the helical structure and the anticancer activity of this series of peptides as *N*-terminal glycine is reported to be abundant in AMPs [42,49,53]. Furthermore, all the peptides were amidated at the C-terminal to increase the positive charge density which is supposed to enhance their anticancer activity [42,52,54]. Although this combination of hydrophobic and cationic amino acids has been previously used for the development of AMPs/ACPs with varying sizes and structures, the newly designed series of anticancer peptides provided in this study have significant structural differences from the previously reported AMPs/ACPs to enhance their anticancer activity and improve their selectivity toward cancer cells. Also, we used a systematic approach by keeping the net positive charge of the peptides constant while changing the amino acid combination in order to investigate the effect of such structural changes on the hydrophobicity and helicity of the peptides and consequently on their anticancer activity/selectivity. Although

α-helical ACPs with various structures have been tested in different cancer cell lines, the anticancer activity of this class of ACPs against colorectal cancer cells has not been reported previously. Another important aspect of our research is studying the anticancer activity of the designed peptides in colorectal cancer 3D multicellular tumor spheroids (MCTSs) which serve as a closer mimic of tumors compared to 2D cell cultures. To the best of our knowledge, there has been very few reports on efficacy of ACPs in MCTSs and none on colorectal cancer MCTSs.

2. Materials & methods

2.1. Materials

The peptides were synthesized by GL Biochem (Shanghai) Ltd and provided as lyophilized powders (Purity > 95%). The peptide solutions were prepared by dissolving the peptide powders in Milli-Q water (Millipore Reagent Water System, USA) and their pH was adjusted to the desirable range using sodium hydroxide. All the chemicals, reagents and organic solvents were sourced from Merck (Sigma Aldrich), UK, with analytical grade. All chemicals had purity ≥ 99 % and all organic solvents had purity ≥ 99.7 %. 1,2-dipalmitoyl-*sn-glycero*-3-phosphocholine (DPPC) and 1,2-dipalmitoyl-*sn-glycero*-3-phospho-(1′-*rac*-glycerol) (DPPG) were purchased from Avanti Polar Lipids (USA), with purity ≥ 99 %. The Dulbecco's Modified Eagle Medium (DMEM), Phosphate buffered saline (PBS), Fetal bovine serum (FBS), Trypsin, Penicillin and streptomycin were all sourced from GIBCO (Thermo Fisher Scientific, UK).

2.2. Determination of peptide sequence and purity

The peptide sequences and molecular weights were verified by Liquid chromatography-Mass spectrometry (LC-MS) (QExactive HF, Thermo Fisher™). The full MS scan from m/z = 375–1500 was acquired in the Orbitrap at a resolution of 120,000. Subsequent fragmentation was Top 2 in the HCD cell, with detection of ions in the Orbitrap using centroid mode, with a resolution of 30,000. The purity of the peptides was checked by reverse phase high performance liquid chromatography (RP-HPLC) using Waters 2695 HPLC system, with Waters 2487 UV/Visible detector set at the wavelength of 205 nm, Xbridge C18 column (4.6 × 250 mm) and a mobile phase consisting of acetonitrile and trifluoroacetic acid (TFA) in water (0.1 % V/V), with a gradient of acetonitrile from 5 to 95% over 20 mins at a flow rate of 1 mL/min.

2.3. Determination of peptide hydrophobicity

The hydrophobicity of the designed cationic amphiphilic peptides was determined both theoretically using the relevant equations and experimentally using RP-HPLC retention times. The mean hydrophobicity value for each peptide was calculated by Eisenberg method [55,56] using the following equation:

$$< H >= \left(\sum_{i=1}^{N} H_i\right)/N \quad (1)$$

Where $< H >$ is the mean hydrophobicity of the peptide sequence, H_i is the hydrophobicity of the ith amino acid in the peptide sequence and N is the number of amino acid residues [55,56]. The values of hydrophobicity for each amino acid were based on the hydrophobicity scale by Fauchère and Pliska which uses the octanol–water partition coefficients [57,58].

2.4. Determination of peptide secondary structure

The secondary structure of the peptides was determined by Circular Dichroism (CD) spectroscopy using a Jasco J-810 spectropolarimeter and a quartz cell of 1 cm path length. The samples were scanned between the wavelength of 190–240 nm with a scanning speed of 100 nm/min and the peptide concentration was fixed at 10 μM. The CD measurements were performed on peptides in aqueous solution and in three different types of curved surfaces: Sodium dodecyl sulfate (SDS) micelles, DPPG small unilamellar vesicles (SUVs) and DPPC SUVs. Each sample was scanned three times and the data were expressed as the average of the three measurements. The mean residue molar ellipticity was calculated using the following equation:

$$\theta_{M=}\frac{\theta_{Obs}}{10}\cdot\frac{M_{RW}}{c\cdot l} \quad (2)$$

Where θ_M is residue molar ellipticity (deg.cm^2.dmol^{-1}), θ_{obs} is the observed ellipticity at a given wavelength (mdeg), M_{RW} is residue molecular weight obtained by dividing the molecular weight of the peptide by the number of amino acid residues, c is the peptide concentration (mg/mL), and l is the path length of the cell (cm) [51,59–62]. The helical content of the peptides was calculated using the following equation:

$$f_H = \left([\theta]_{222} + 2000\right)/[\theta]^H_{222} \quad (3)$$

Where f_H is the fraction of helix, $[\theta]_{222}$ is the measured mean residue molar ellipticity at 222 nm, and $[\theta]^H_{222}$ is the mean residue molar ellipticity for 100% helical content at 222 nm which in this case was −28400 deg.cm^2.dmol^{-1} based on the length of the peptides [61–64].

2.5. Preparation of lipid vesicles

The DPPC and DPPG SUVs were prepared by the thin-film hydration method. The lipids were dissolved in chloroform at a concentration of 2 mg/mL, then the solvent was evaporated under vacuum using a rotary evaporator (Heidolph Instruments GmbH & CO). The resulting thin lipid film was rehydrated with phosphate buffer (pH = 7.4) and then brought to the desired size by extrusion using Avanti mini-Extruder (Avanti Polar Lipids, USA) containing a polycarbonate membrane with a pore size of 200 nm. The SDS micelles were simply prepared by dissolving SDS powder in Milli-Q water at the concentration of 25 mM which is above the critical micelle concentration of SDS. The size of the lipid vesicles was measured by Dynamic Light Scattering (DLS) using ZetaPALS zeta potential analyzer, Brookhaven instruments corporation, and reported as the average of 6 scans.

2.6. Surface activity and interaction of the peptides with lipid monolayers

The surface pressure measurements were performed using a Langmuir trough (NIMA technology Ltd, Coventry, UK), with a 3 mL built-in Teflon trough and a Wilhelmy plate attached to the pressure sensor. The trough was filled with 3 mL of PBS (pH = 7.4), the peptide solution was injected underneath the buffer surface using a Hamilton microsyringe and the changes to the surface pressure at the air–water interface was recorded as a function of time for 2 h. The surface activity of the peptides upon adsorption at the air/water interface results in a decrease in the surface tension from that of pure water. The surface pressure (π) is defined as the difference between the initial surface tension (γ_0) of the pure water and the final surface tension (γ) following adsorption of the peptides at the air/water interface [40,65]:

$$\pi = \gamma_0 - \gamma \quad (4)$$

The interaction of the peptides with the lipid monolayers was studied by monitoring the changes to the surface pressure of lipid monolayers made of DPPG or DPPC. The lipid monolayers were formed by spreading the lipid solution in chloroform (0.5 mg/mL) at the air-buffer interface using a Hamilton microsyringe. After allowing 20 min for the solvent to evaporate and the lipid monolayer to equilibrate, the peptide solution was injected underneath the monolayer into the subphase with a final concentration of 20 μM and the changes to the surface pressure over time were monitored for 2 h. The initial pressure of the lipid monolayer was set to 28 mN/m which is close to the average cell membrane resting pressure [42,54,66]. All the measurements were performed in triplicate and the values were reported as the average of the three runs.

2.7. Cytotoxicity tests

The cytotoxicity tests were performed in three different human cell lines, HCT 116 colorectal adenocarcinoma cells, HeLa cervical cancer cells, and Human dermal fibroblasts (HDFs). All cells were cultured in DMEM enriched with 10% FBS and 1% antibiotic (100 U/mL penicillin and 100 μg/mL streptomycin) at 37 °C under 5% CO_2. The cytotoxicity of the peptides in different cell lines was assessed by MTT assay. The cells were cultured in 96 well plates at a seeding density of 4000 cells/well and incubated with different concentrations of the peptide solutions at 37 °C. After 72 h the cells were subjected to MTT assay following the standard protocols. Briefly, 10 μL of MTT solution (5 mg/mL) was added to each well and incubated at 37 °C for 4 h. Subsequently, the cell culture media was replaced with Dimethyl Sulfoxide (DMSO). The plates were shaken for 15 min to allow for complete dissolution of the precipitated formazan dye and then the absorbance of formazan was measured at 590 nm using a microplate reader (Varioskan Flash™, Thermo Fisher Scientific). Data were normalised using the absorbance of untreated cells as controls. All experiments were repeated 6 times and the values were reported as Mean ± SE.

The cytotoxicity of the peptides in different cell lines was further investigated by cell proliferation assay. The cells were cultured under the same experimental conditions described for MTT assay, and incubated with the peptides (100 μM) for 72 h. Subsequently, the cells were stained with Hoechst 33342 and Flash Phalloidin™ Red 594 and imaged using high content fluorescent automated widefield microscope (ImageXpress® Micro System, Molecular Devices, USA). In order to evaluate the cytotoxicity of the cationic amphiphilic peptides in multicellular tumour spheroids (MCTSs) HCT 116 cells were cultured in ultra-low binding 96 well plates at a seeding density of 10,000 cells/well. The cells were incubated for 24 h to allow for the formation of MCTSs, then treated with the cationic amphiphilic peptides (at the concentration of 100 μM) and incubated for 72 h. Anticancer activity was evaluated in terms of reduction in the size of the MCTSs as visualized by brightfield microscopy. The MCTSs were also stained with live-dead assay kit consisting of propidium iodide and Syto 9 and then imaged by high content microscope.

2.8. Mitochondrial damage tests

The ability of the cationic amphiphilic peptides to damage the mitochondrial membrane was assessed using JC-1 mitochondrial probe (Invitrogen™). The cells were cultured in 96 well plates at a seeding density of 4000 cells/well and incubated with the peptide solutions (20 μM) for 72 h. Subsequently, the cells were stained with JC-1 following the manufacturer's protocol. Briefly, the cells were washed with PBS, then prewarmed (37 °C) fresh media containing JC-1 (10 μg/mL) was added to the cells (100 μL/well) and incubated at 37 °C for 15 min after which the media was removed, the cells were washed again with PBS and then submerged in PBS (100 μL/well). The live imaging was performed using high content microscope with CY3 and FITC filters for the red and green fluorescence emission respectively.

2.9. Data analysis

The quantitative data were analysed using Microsoft® Excel 2016 and GraphPad Prism 8. All data were reported as Mean ± SD or Mean ± SE of the repeats. For the correlation graphs the data were subjected to linear regression analysis at 95% confidence interval ($\alpha = 0.05$) and values of $p < 0.05$ were used to determine the goodness of fit. The microscopic images were analysed using MetaXpress® software 5.3.01 (Molecular Devices, USA).

3. Results and discussion

3.1. Structures and physicochemical properties of the designed peptides

The full peptide sequences and molecular weights are provided in Table 1. The peptide sequences were confirmed by LC-MS and the molecular weights measured by LC-MS were very close to the theoretical molecular weights calculated for these peptide sequences.

As can be seen from Table 1, the calculated mean hydrophobicity values of the designed ACPs suggest a minor decrease to the peptide hydrophobicity upon replacing lysine with arginine but a more significant reduction in the hydrophobicity upon replacement of isoleucine with leucine. On the contrary, the RP-HPLC retention times indicated a different trend in the hydrophobicity of the designed ACPs as both replacing lysine with arginine and replacing isoleucine with leucine increased the hydrophobicity and consequently the retention times of the peptides. This inconsistency between the theoretically predicted and the experimentally measured hydrophobicity lies in the fact that the mean hydrophobicity of a peptide is merely based on its amino acid composition and does not take into account other factors such as the secondary structure. On the other hand, the RP-HPLC retention times provide a more accurate real-time measure of the peptide hydrophobicity as they reflect the strength of the interaction between the peptide and the stationary phase [40,67–71]. It has been well evidenced that the hydrophobic surface of the RP-HPLC stationary phase (the C18 column) induces α-helical conformation in the peptide chain which in return leads to stronger binding of the nonpolar face of the α-helix to the column and a substantial increase in the retention times compared to that predicted using amino acid-based partition coefficients [40,67–71]. Hence the higher hydrophobicity of the arginine-rich or leucine-rich peptides is likely to be due to stronger α-helical conformation upon contact with the hydrophobic surface of the stationary phase which is in accordance with the observed helical content of these peptides as determined by circular dichroism (Section 3.2). Similar observations have been reported by other studies showing poor correlation between the theoretically computed hydrophobicity of the α-helical peptides and the experimental hydrophobicity measured by RP-HPLC indicating lack of accuracy of the theoretical calculation method and suggesting the RP-HPLC retention times as a more realistic and accurate measure of the peptide hydrophobicity [40,61,70,71].

Table 1
Sequences and chemical properties of the designed cationic amphiphilic peptides.

Peptide	Sequence	Charge	Theoretical MW[a]	Measured MW[b]	RT[c]	<H>[d]
IK-13	CIIKKIIKKIIKK-NH_2	+6	1568.2	1568.1	10.0	0.49
LK-13	CLLKKLLKKLLKK-NH_2	+6	1568.2	1568.1	10.8	0.45
IR-13	CIIRRIIRRIIRR-NH_2	+6	1736.2	1736.3	9.5	0.48
LR-13	CLLRRLLRRLLRR-NH_2	+6	1736.2	1736.3	11.3	0.44
CI-15	CIIKKIIKKIIKKII-NH_2	+6	1794.4	1795.4	11.9	0.67
GI-15	LC-Propargyl-GIIKKIIKKIIKKII-NH_2	+6	1786.4	1786.7	11.7	0.56

a, the theoretical molecular weights as calculated using the online tool from the website "https://pepcalc.com"; b, the real molecular weights as measured by LC-MS; c, the HPLC retention times; d, the mean hydrophobicity values calculated by Eisenberg method using the hydrophobicity scale defined by Fauchère and Pliska.

3.2. Secondary structure of the peptides

The CD spectra of the designed ACPs in aqueous solution and upon contact with different types of curved hydrophobic surfaces are provided in Fig. 1. As can be observed, all of the designed peptides were unfolded in aqueous solution as denoted by the presence of a negative peak at 198–200 nm which is indicative of random coil structure [39,40,42,62,72,73]. This is attributed to the strong intermolecular hydrogen bonding between the peptides and the water molecules as well as the electrostatic repulsion between the adjacent positively charged arginine/lysine residues [40,74]. However, upon contact with the curved hydrophobic surfaces (phospholipid SUVs or SDS micelles), the peptides adopted α-helical structure denoted by a positive peak at 193 nm and negative peaks at 208 nm and 220–222 nm [39,40,42,59,62,73]. Although different peptides showed different degree of helicity in different environments, they all showed a higher tendency for forming α-helical structure in the anionic environment of DPPG SUVs and SDS micelles compared to the zwitterionic environment of DPPC SUVs except for IR-13. This is attributed to the cationic nature of the peptides which favours interaction with the anionic lipid bilayers over zwitterionic lipid bilayers. As a result, the polar surface of the α-helix interacts with the hydrophilic heads of the phospholipids or SDS through charge interaction and the nonpolar surface of the α-helix is inserted into the lipid bilayer [40]. These results are in agreement with the literature data reported for other types of short cationic amphiphilic α-helical AMPs/ACPs and also cell penetrating peptides (CPPs) which have unfolded random coil structure in aqueous solution but fold into α-helix in SDS micelles or negatively charged phospholipid vesicles such as DOPG and DPPG [39,40,42,62,73,74].

The separation between the polar and nonpolar faces of the α-helix could be well portrayed using the Schiffer-Edmundson Helical wheel projections (Fig. 1F). The helical wheels provide a two-dimensional projection of the α-helix with separate hydrophobic and hydrophilic surfaces [75]. The helical content of the peptides in different types of hydrophobic curved surfaces could be compared using the observed mean residue molar ellipticity at 222 nm (Fig. 1). Comparison of the helical content of different cationic amphiphilic peptides in phospholipid bilayers revealed that CI-15 and GI-15 had the highest helical content in DPPG SUVs which indicates the role of the additional C-terminal isoleucine in increasing the helical propensity of the peptide. The lower helicity of GI-15 compared to CI-15 is supposed to be due to the presence of LC-Propargylglycine instead of Cysteine in the *N*-terminal which disfavours the helical formation. Similar findings have been reported by Chen et al with regard to other short cationic amphiphilic AMPs indicating the favourable effect of C-terminal isoleucine and unfavourable effect of *N*-terminal glycine on the formation and stabilization of the α-helical structure [52]. The trend observed for the increase in helicity of the ACPs in SDS micelles and DPPG SUVs was consistent with the trend observed for the increase in RP-HPLC retention times (Fig. 1 G-H). The good correlation between the helical content in curved hydrophobic surfaces and the retention times further confirms the significant effect of the conformational change from random coil into α-helix upon interaction with the hydrophobic surface of the stationary phase

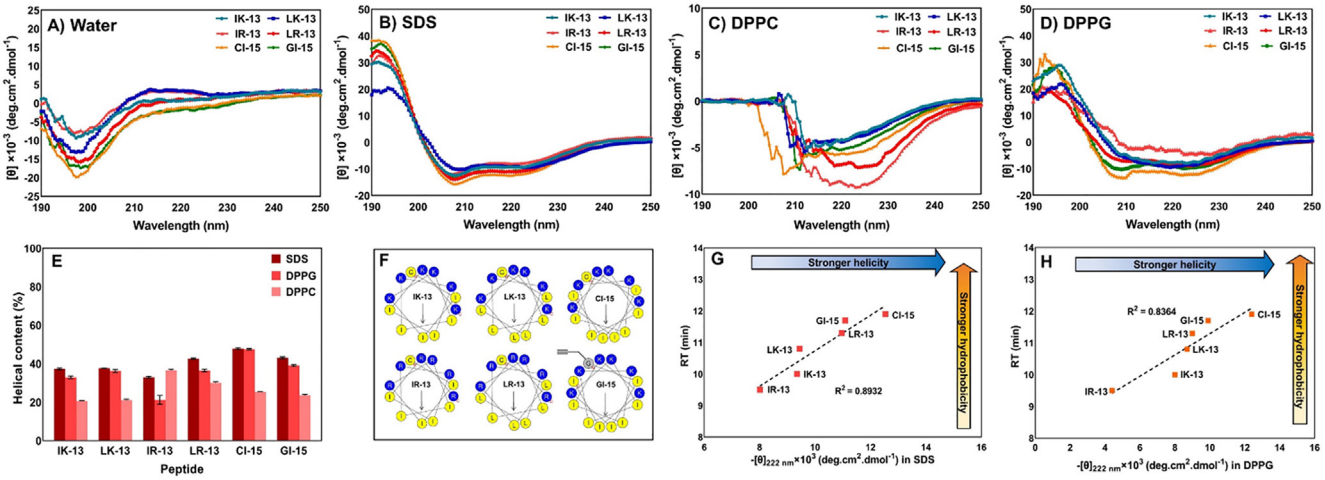

Fig. 1. Secondary structure of the peptides. Circular dichroism spectra of the cationic amphiphilic peptides in DI water (**A**), SDS micelles (**B**), DPPC SUVs (**C**) and DPPG SUVs (**D**). The data are reported as the average of 3 repeats. Helical content of the peptides in SDS, DPPC and DPPG SUVs (**E**). Schiffer-Edmundson Helical wheel projections of the designed cationic amphiphilic peptides (**F**). The blue circles represent hydrophilic amino acids (K and R) and the yellow circles represent hydrophobic amino acids (I, L and C). Drawn using the online tool of the website "https://heliquest.ipmc.cnrs.fr/cgi-bin/ComputParams.py". Correlation between the degree of helicity of the peptides in SDS micelles (**G**) or DPPG SUVs (**H**) and their apparent hydrophobicity as measured by RP-HPLC retention times.

on the apparent hydrophobicity of the cationic amphiphilic peptides as reported elsewhere [40,61,71].

3.3. Cytotoxicity of the ACPs in normal and cancer cells

The cytotoxicity of the designed ACPs against cancer cells and normal cells as determined by MTT assay are presented in Fig. 2 and the values of half maximal inhibitory concentration (IC_{50}) calculated using the concentration–response curves are provided in Table 2. As it could be observed, there was a marked difference between the cytotoxicity of the cationic amphiphilic peptides in cancer cell lines (HCT 116 and HeLa) and human dermal fibroblasts (HDF). IK-13, CI-15 and GI-15 were considerably more toxic to cancer cells compared to fibroblasts, indicating their selective anticancer activity, whereas IR-13 and LR-13 were highly toxic to fibroblasts. Thus, replacing the lysine residues with arginine residues in the hydrophilic domain of the designed ACPs increased their toxicity against normal cells. Moreover, in the case of IR-13, it also diminished its toxicity against cancer cells. LK-13 was selectively toxic to HCT 116 but had very poor toxicity against HeLa suggesting the importance of the isoleucine residues in the hydrophobic domain for toxicity against HeLa. These observations suggest the importance of scanning different ACPs in different cancer cell lines for optimising the anticancer effect of the ACPs. The strong anticancer activity of CI-15 and GI-15 compared to the other peptides in this series is mainly attributed to the presence of the additional isoleucine residues in their C-terminal resulting in higher helical content in anionic environments such as negatively charged cancer cell membranes which can increase their cell penetration. The higher overall hydrophobicity of these peptides could also favour their penetration into the lipid bilayer of the cell membrane. Comparing the anticancer activity of the designed peptides with literature data revealed similar anticancer activity against HeLa cells exerted by GI-15 and a peptide with closely related structure designed by Chen et al [42,54], named G_3, with the sequence $G(IIKK)_3I\text{-}NH_2$ (IC_{50}: 16.6 μM vs. 15–16 μM for GI-15 and G_3 respectively). On the other hand, CI-15 exhibited 5 times higher anticancer potency against HeLa cells compared to G_3 (IC_{50}: 2.7 μM vs. 15–16 μM for CI-15 and G_3 in order) while still maintaining low toxicity against fibroblasts. Hence, replacing the *N*-terminal glycine with Cysteine enhances the anticancer activity of this group of peptides while maintaining their selectivity for cancer cells.

Table 2
Half maximal inhibitory concentration (IC_{50}) values of the designed cationic amphiphilic peptides in different cell lines as determined by MTT assay. All values are reported as Mean ± SD of 6 replicates.

Peptide	IC_{50} (μM)		
	HCT 116	HeLa	HDF
IK-13	29 ± 6	47 ± 5	> 100
LK-13	23 ± 2	83 ± 9	> 100
IR-13	> 100	> 100	22 ± 3
LR-13	15.6 ± 1.0	26.7 ± 1.3	24 ± 5
CI-15	7.7 ± 0.2	2.7 ± 0.5	83 ± 5
GI-15	13.6 ± 0.2	16.6 ± 0.8	81 ± 8

The selective cytotoxicity of the designed ACPs towards HCT 116 and HeLa was further confirmed by cell proliferation assays demonstrating a reduction in the cell population of the cancer cells treated with IK-13, LK-13, CI-15 and GI-15 compared to the untreated controls and also changes to the morphology of the cells (shrinkage of the pre-apoptotic cells) whereas the HDF cells were less affected by the ACPs (Fig. 3). In a similar fashion to the MTT assay, CI-15 and GI-15 were found to be equally effective against both HCT 116 and HeLa whereas IK-13 and LK-13 were more effective against HCT 116. IR-13 which lacked any significant anticancer activity in the experimental range of concentrations and LR-13 which lacked any selectivity for cancer cells were not included in this experiment.

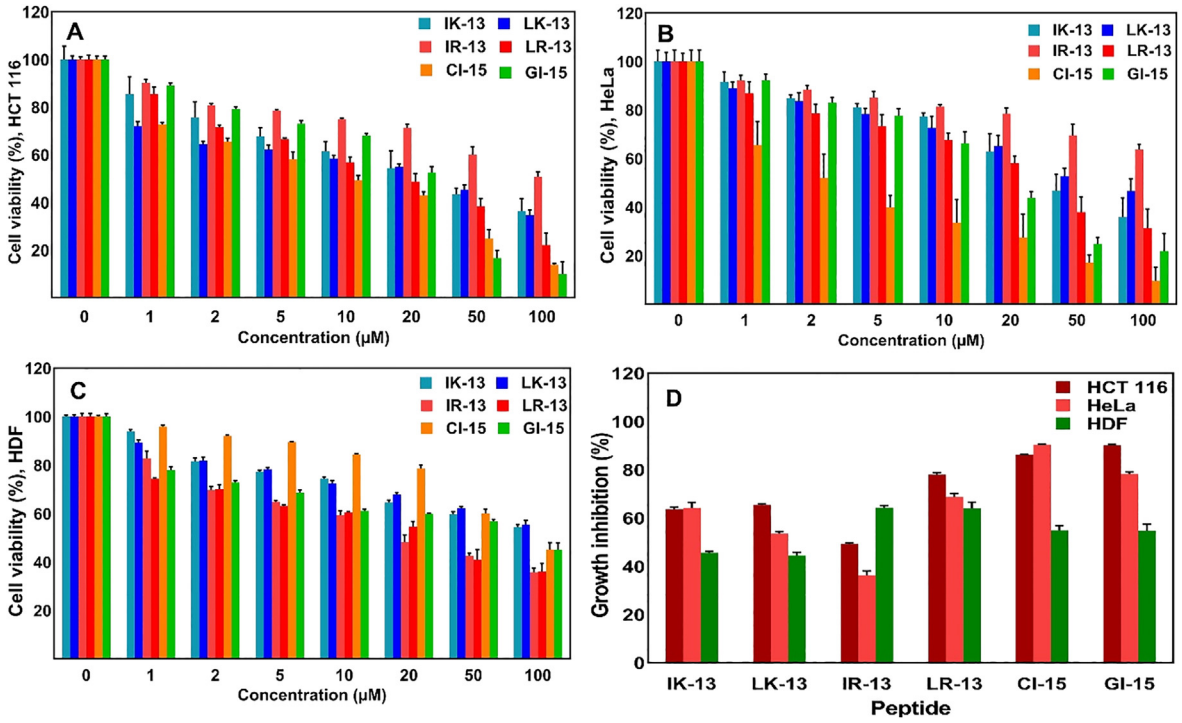

Fig. 2. Cytotoxicity of the cationic amphiphilic peptides in HCT 116 (**A**), HeLa (**B**), and HDF (**C**) as determined by MTT assay. (**D**) Maximum growth inhibition achieved by the cationic amphiphilic peptides (at the concentration of 100 μM) in different cell lines. All values were normalized compared to the untreated controls and reported as Mean ± SE of 6 repeats.

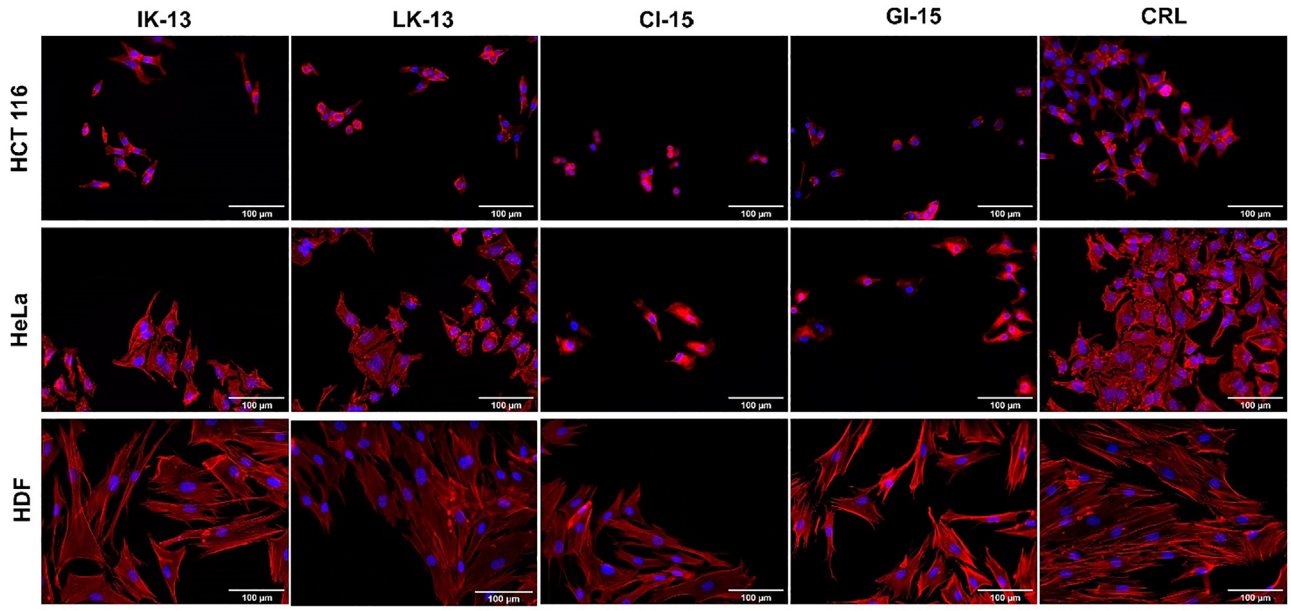

Fig. 3. High content images of HCT 116, HeLa, and HDF cells treated with the anticancer peptides (100 μM for 72 h) compared to the untreated controls (CRL). The nuclei are stained with Hoechst 33342 (blue) and actin is stained with Phalloidin (red). × 20 magnification, scale bar: 100 μm.

The role of hydrophobicity and helicity of the peptides in determining their anticancer activity/selectivity is further visualized by the correlation plots depicted in Fig. 4. As it could be observed, there was a strong correlation between the anticancer activity of the peptides in HCT 116 and their helical content in the negatively charged DPPG lipid bilayers which mimic the cancer cell membranes. Similarly, the cytotoxicity of the peptides against HDF was well correlated to their helical content in the zwitterionic DPPC lipid bilayers which are a mimic of the normal mammalian cell membranes. This is in agreement with the results reported

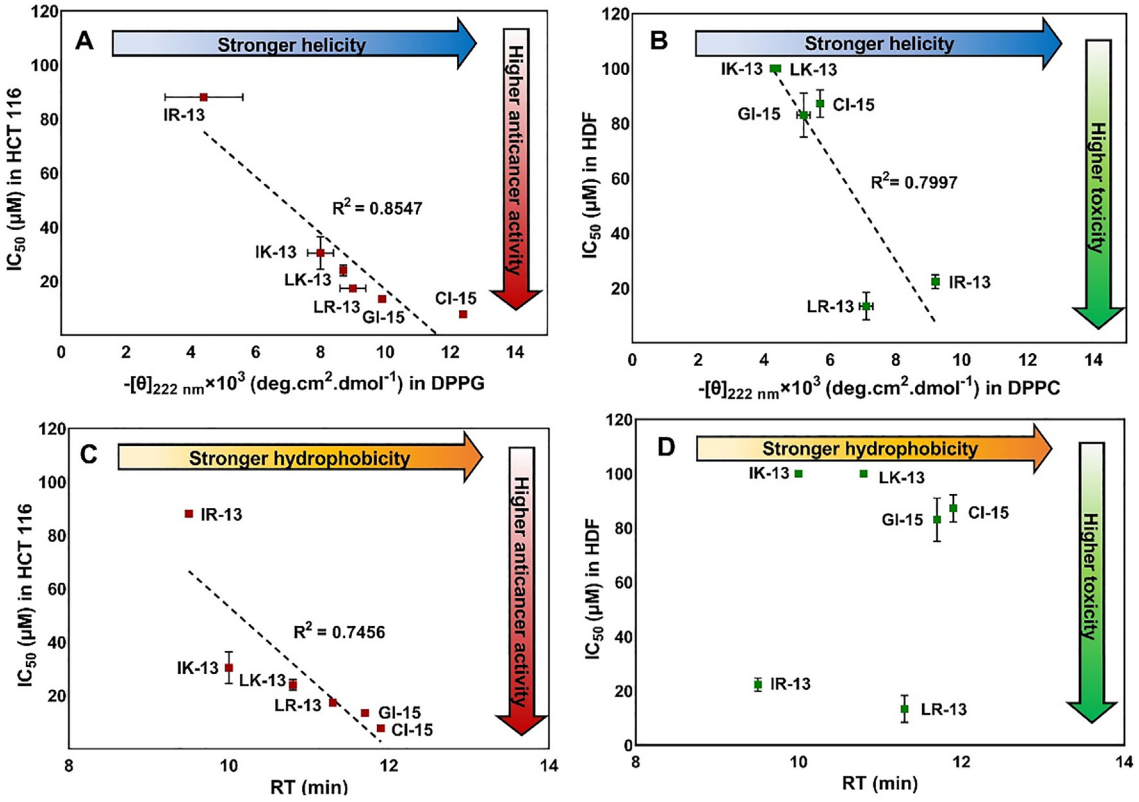

Fig. 4. Correlation between the cytotoxicity of the cationic amphiphilic peptides in HCT 116 (**A**) and HDF (**B**) and their helical content in DPPG and DPPC SUVs, respectively. Relationship between the cytotoxicity of the cationic amphiphilic peptides in HCT 116 (**C**) and HDF (**D**) and their hydrophobicity as determined by RP-HPLC retention times. The values of half maximal inhibitory concentration (IC_{50}) were reported as the average of 6 repeats and the values of mean residue molar ellipticity (θ) were reported as the average of 3 repeats.

by Chen et al for anticancer peptides with closely related structures, named G_3 and G_4, with the sequences G(IIKK)$_3$I –NH_2 and G(IIKK)$_4$I-NH_2 respectively [54]. Similar results were reported by Gong et al for another group of ACPs derived from G_3 (i.e., G(ILKK)$_3$I-NH_2, G(IVKK)$_3$I-NH_2, G(IVKO)$_3$I-NH_2) [39].

The cytotoxicity of the cationic amphiphilic peptides in HCT 116 was also very well correlated with their hydrophobicity and the more hydrophobic peptides exhibited the strongest anticancer activity. This is consistent with the studies by Kim et al [70] and Gong et al [39] who reported a strong correlation between the hydrophobicity of the α-helical AMPs, as determined by their RP-HPLC retention times, and their antimicrobial activity [39,70]. In HDF cells, on the other hand, there was a poor correlation between hydrophobicity and cytotoxicity, and no specific pattern was observed. Nevertheless, a closer look at the plot reveals that the cytotoxicity of the lysine-rich peptides against fibroblasts increased with their hydrophobicity although the differences were not significant. Hence, it could be deducted from these data that the anticancer activity of the designed cationic amphiphilic peptides is determined by both their hydrophobicity and their helical content whereas their selectivity towards cancer cells is mainly a function of their helical content in the zwitterionic membrane of the normal cells and hydrophobicity plays a minor role in it.

3.4. Cytotoxicity of the ACPs in 3D multicellular tumour spheroids (MCTSs)

Following cytotoxicity tests in 2D cell culture, the anticancer activity of the designed cationic amphiphilic peptides was further assessed in 3D MCTSs made of HCT 116 as a mimic of colorectal adenocarcinoma. MCTSs mimic the 3D cellular context of the solid tumours and possess features resembling *in vivo* tumours such as cell-to-cell contact, excretion of extracellular matrix (ECM), development of pH, oxygen and metabolic gradients [76–79]. Therefore, they are superior to 2D cell culture systems in reflecting the tumour tissue's response to drugs and bridge the gap between the 2D cell culture and animal models [77–79]. Although 3D MCTSs have been used for evaluating the efficacy of conventional anticancer drugs, there have been very few reports on the efficacy of anticancer peptides in MCTSs which has been limited to melanoma, glioblastoma and lung tumour MCTSs [80–84]. To the best of our knowledge, this is the first study on the efficacy of ACPs in colorectal adenocarcinoma MCTSs.

As it could be observed in Fig. 5, two of the designed peptides, CI-15 and GI-15, which had the strongest anticancer effect against HCT 116 in 2D cell culture also exhibited considerable anticancer activity in HCT 116 MCTSs manifested by a significant reduction in the spheroid size and presence of more dead cells in the spheroid core compared to untreated spheroids. The other peptides were unable to induce any apparent cytotoxicity in MCTSs at the experimental condition. It is also noteworthy that the concentration of the ACPs required for achieving an observable anticancer effect in 3D MCTSs was significantly higher than that required for 2D cell culture. Hence, lack of anticancer activity in MCTSs by IK-13 and LK-13 could be attributed to the weaker anticancer activity of these two peptides compared to CI-15 and GI-15 based on their IC_{50} values in HCT 116. It is supposed that for these peptides to be able to exhibit any apparent anticancer activity in MCTSs, considerably higher concentrations may be required.

3.5. Surface activity of the cationic amphiphilic peptides determines their anticancer activity

The amphiphilic activities of the designed ACPs were further measured by their surface adsorption at the air/water interface, which resulted in a decrease in the surface tension from that of pure water/buffer, defined as surface pressure, which is indicative of the surface activity of the peptides. The surface activity experiments were only performed on the peptides with higher selectivity for cancer cells. Nevertheless, IR-13 which had poor anticancer activity was also tested as a negative control for comparison. As it could be observed in Fig. 6A, adsorption of the ACPs at the air–water interface resulted in increased surface pressure the extent of which was directly proportional to the concentration of the peptides in the subphase. Thus, the observed interfacial adsorption of the peptides was concentration dependent. The increase in the surface pressure upon interfacial adsorption of the ACPs was in line with their anticancer activity. The peptides with stronger anticancer activity gave rise to higher surface pressure (Fig. 6) while IR-13, which has poor anticancer activity, induced considerably lower surface pressure than other peptides. There was a strong correlation between the increase in surface pressure by the ACPs and their helical content in SDS micelles (R^2 = 0.73) suggesting that the same conformational changes that occur at the curved oil–water interface of the SDS micelles may occur upon adsorption of the peptides at the air/water interface. These conformational changes allow for orientation of the hydrophilic surface of the α-helix in the aqueous subphase and projection of the hydrophobic surface of the α-helix outside the water in the air. Similar observations have been reported by other studies with other types of α-helical cationic amphiphilic peptides [42,85]. The surface pressure of the ACPs at the air/water interface was also well correlated with their hydrophobicity (R^2 = 0.79). Hence, the surface pressure of the α-helical peptides at the air–water interface is governed by an interplay between their hydrophobicity and their helical content.

3.6. Penetration of the cationic amphiphilic peptides into lipid monolayers as a mimic of normal and cancer cell membranes

As mentioned earlier, it is generally believed that the mechanism of selectivity of the ACPs for cancer cells is mainly via targeting the cancer cell membranes. In order to confirm that the observed selectivity of the designed ACPs for cancer cells lies in their higher affinity for cancer cell membranes, the anionic DPPG monolayers and the zwitterionic DPPC monolayers were used as *in vitro* models of the outer leaflet of cancer and normal cell membranes respectively [54,66,86,87]. The insertion of the cationic amphiphilic peptides into lipid monolayers was studied by monitoring the changes to the surface pressure over time following injection of the peptide solution under the lipid monolayer at a constant surface area. The experiments were performed at an initial surface pressure of 28 mN/m which is close to the resting pressure of the mammalian cell membrane [42,54,66]. The peptides with higher selectivity for cancer cells (IK-13, LK-13, CI-15, and GI-15) were included in these experiments to investigate the correlation between their biological activity and their interfacial behaviour.

As it could be observed in Fig. 7, the peptides exhibited a greater tendency to interact with the anionic DPPG monolayer compared to the zwitterionic DPPC monolayer except for IR-13 which showed a preference for DPPC over DPPG. It is suggested that the stronger electrostatic interaction between the cationic peptides and the anionic phospholipids facilitates their insertion into the DPPG lipid monolayer. The binding of the short cationic amphiphilic peptides to the lipid monolayers involves two steps; initial binding/adsorption of the peptide to the lipid monolayer happens through electrostatic interactions between the positively charged amino acid residues and the negatively charged phospholipid headgroups. Subsequently, hydrophobic interactions between the hydrophobic amino acid residues and the acyl chains of the phospholipid disturbs the acyl chain ordering and results in increased surface pressure [85,88].

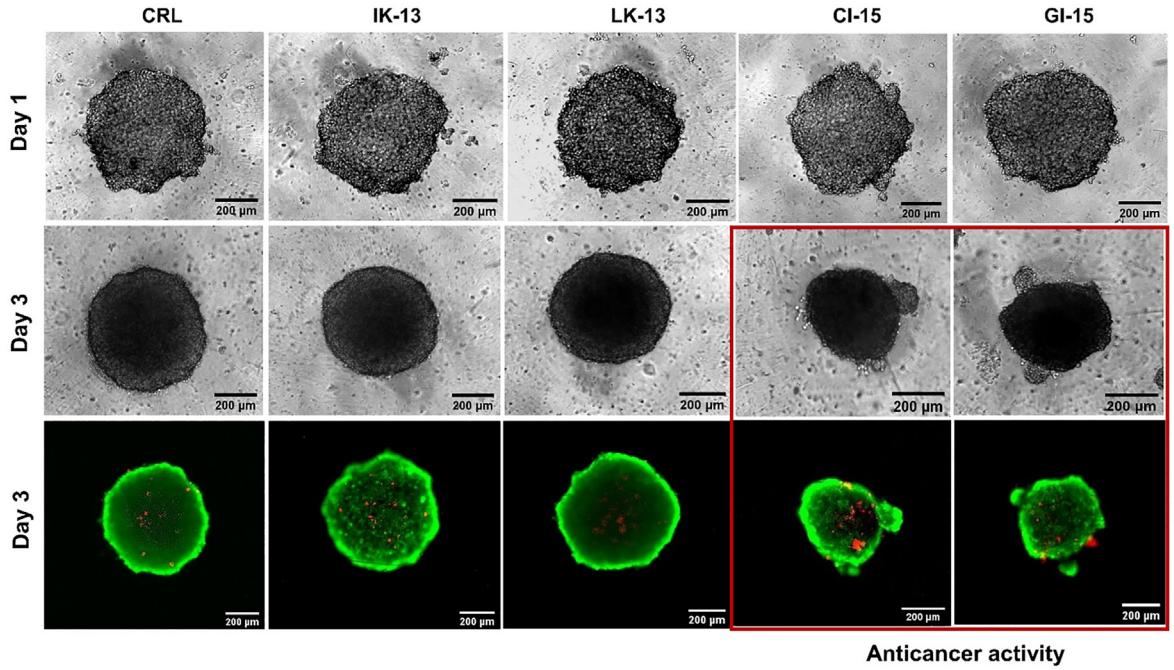

Fig. 5. Cytotoxicity of the anticancer peptides in HCT 116 multicellular tumour spheroids (MCTSs). The green colour (Cyto 9) marks the healthy cells, and the red colour (propidium iodide) indicates the dead cells.

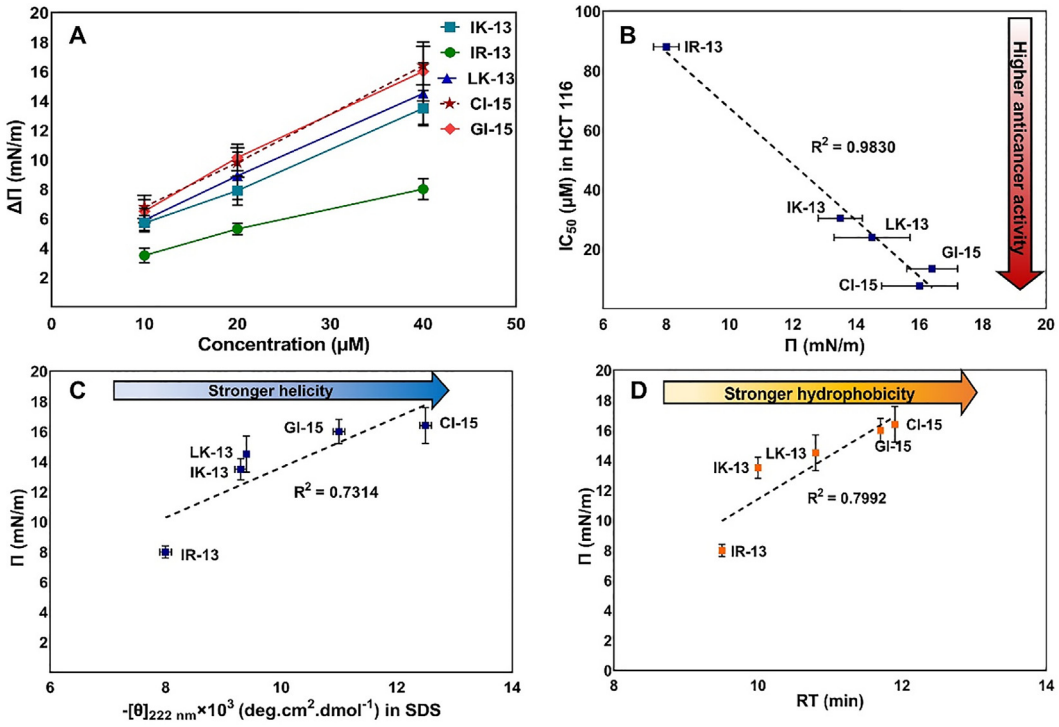

Fig. 6. Increase in surface pressure at the air- water interface following injection of different concentrations of cationic amphiphilic peptides (**A**). Correlation between the anticancer activity of the cationic amphiphilic peptides in HCT 116 and increase in surface pressure upon adsorption of the peptides (at the concentration of 40 µM) at the air water interface (**B**). Correlation between the surface pressure of the cationic amphiphilic peptides and their helical content in SDS micelles (**C**). Correlation between the surface pressure of the cationic amphiphilic peptides and their hydrophobicity as determined by RP-HPLC retention times (**D**). The values of pressure (π) and mean residue molar ellipticity (θ) are reported as the average of 3 repeats. The values of half maximal inhibitory concentration (IC_{50}) are reported as the average of six repeats.

The observed trend for the increase in the surface pressure of the DPPG lipid monolayers upon interaction with the ACPs was consistent with the observed anticancer activity of the peptides (R^2 = 0.99). Similarly, a good correlation was found between the toxicity of the peptides in HDFs and the increase in the surface pressure upon injection of the peptides under DPPC lipid monolayers (R^2 = 0.89). The order of increase in the surface pressure following interaction of the ACPs with DPPG monolayer was directly

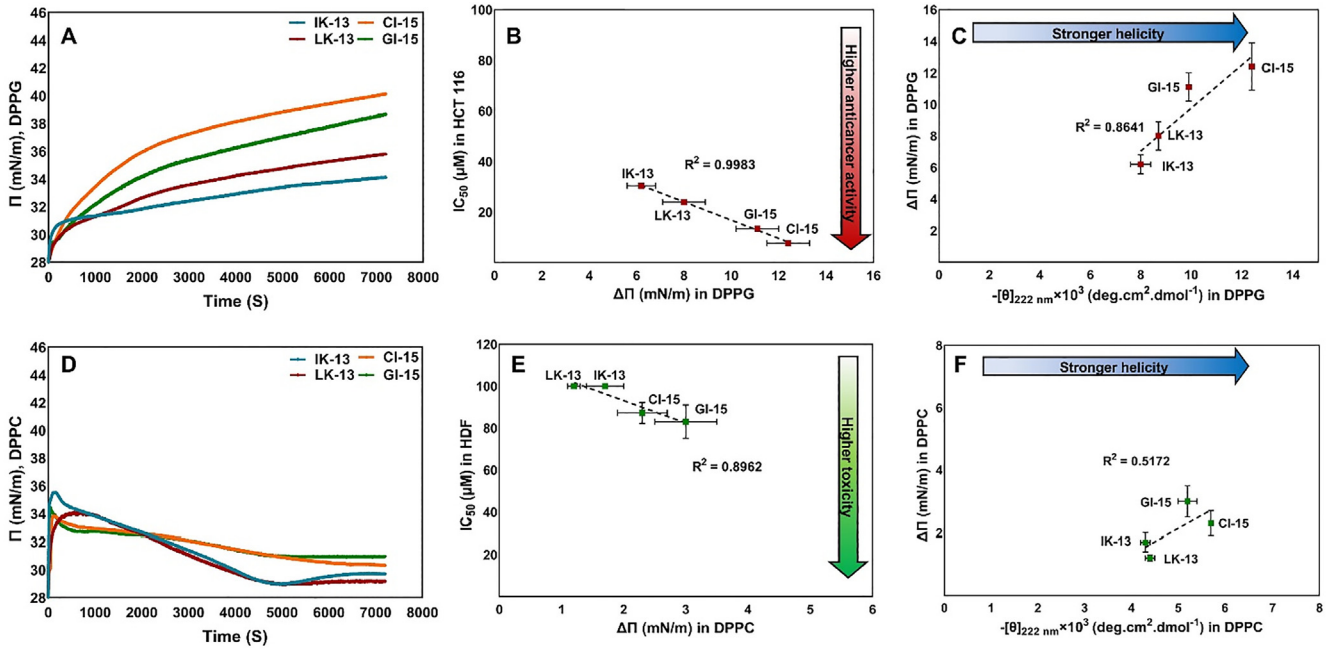

Fig. 7. (A, D) Increase in the pressure of the DPPG and DPPC lipid monolayers upon injection of the cationic amphiphilic peptides (at the concentration of 20 μM) in the subphase. **(B, E)** Correlation between cytotoxicity of the ACPs in HCT 116 or HDF and increase in the surface pressure of DPPG or DPPC lipid monolayers, respectively. **(C, F)** Correlation between the increase in the surface pressure of DPPG and DPPC lipid monolayers upon injection of the ACPs and the peptide helicity in DPPG and DPPC SUVs, respectively. The values of pressure (π), increase in pressure ($\Delta\pi$), and mean residue molar ellipticity (θ) are reported as the average of 3 repeats. The values of half maximal inhibitory concentration (IC_{50}) are reported as the average of 6 repeats.

proportional to their helicity in DPPG SUVs (R^2 = 0.86). Hence, it is suggested that similar conformational changes that occur upon contact of the ACPs with DPPG lipid bilayers may also happen upon their contact with DPPG lipid monolayers facilitating their penetration into the DPPG monolayer. Another factor contributing to the higher adsorption and subsequently penetration of CI-15 and GI-15 into the DPPG monolayers compared to the other peptides of shorter length in this group could be the decreased entropy per amino acid as it has been evidenced that unlike the proteins, for the peptides the entropy penalty for binding to lipid mono and bilayers is decreased by increasing the length of the peptide [89,90].

On the other hand, although the ACPs with low toxicity in HDFs generally had low helical content in DPPC SUVs and low surface pressure upon interaction with DPPC lipid monolayers, the relationship between their helicity and their surface pressure in DPPC was not linear. It is therefore supposed that the interaction of the designed ACPs with the zwitterionic DPPC lipid monolayers is more directed by the hydrophobic interactions between the hydrophobic domain of the peptide and the acyl chains of the phospholipids and the conformational change plays a less important role in it.

Overall, the lower values of pressure in DPPC monolayers compared to DPPG monolayers indicates weaker interactions of the peptides with the zwitterionic lipids. These observations further confirm the previously mentioned hypothesis that the penetration of the cationic amphiphilic peptides into the phospholipid monolayers is a two-step process and that the stronger electrostatic interactions between the positively charged peptides and the negatively charged headgroups of DPPG compared to the zwitterionic headgroups of DPPC plays an important role in higher affinity of the peptides for penetration into DPPG lipid monolayers. Although the lipid monolayers are limited in providing information about the exact mechanism of material transport across the cell membrane as they only serve as a model for the outer leaflet of the cell membrane, the suggested adsorption mechanism and the conformational changes associated with penetration of the ACPs into the phospholipid monolayers are considered to be essential for the subsequent translocation of the peptides across the cell membrane and to direct the cellular uptake of the peptides by different types of cells.

3.7. Higher cellular uptake of the cationic amphiphilic peptides by cancer cells compared to normal cells indicates their selectivity for cancer cells

The cell membrane disruption resulting from interaction of the ACPs with the phospholipids in the cell membrane, eventually dictates the extent of cell penetration of the peptides. The weak interaction of the cationic amphiphilic peptides with the cell membrane of normal cells leads to low cellular uptake of these peptides which could be one of the reasons for the lower toxicity of these peptides in normal cells compared to cancer cells. To confirm this assumption, the cationic amphiphilic peptide GI-15 labelled with the fluorescent probe Alexa Fluor™ 594 was added to HCT 116 and HDF cells and its cellular uptake was tracked. As it could be observed in Fig. 8, the higher intensity and greater distribution of the red fluorescence in the cytoplasm of HCT 116 cells compared to HDF cells provides compelling evidence for higher cellular uptake of the peptide by HCT 116 compared to HDF. Hence, the charge difference between the cancer cell membranes and normal cell membranes not only provides a basis for cancer cell targeting but also leads to increased intracellular concentrations of the peptides in cancer cells compared to normal cells, which in return reduces the amount of peptide required for achieving cytotoxicity as reflected by lower values of IC_{50} for the peptides in cancer cells compared to fibroblasts. These observations further indicate the increased peptide transport across the anionic membrane of the cancer cells which is in agreement with the higher binding affinity and higher

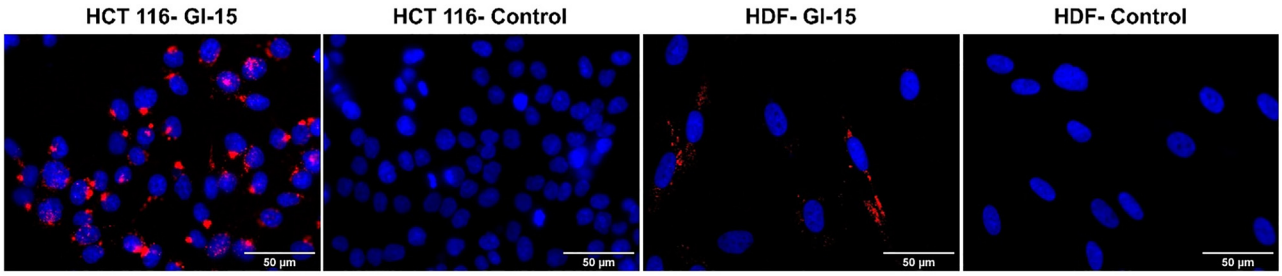

Fig. 8. Cellular uptake of Alexa Fluor™ 594 labelled GI-15 (red) in HCT 116 and HDF cells compared to untreated controls. The nuclei are stained with Hoechst 33342 (blue).

penetration of the peptides in DPPG lipid monolayers as discussed in Section 3.6.

3.8. The cationic amphiphilic peptides exert their cytotoxicity by damaging the mitochondria

In order to unravel the mechanism of anticancer activity of the designed ACPs, their interaction with the mitochondrial membranes was investigated by assessing the mitochondrial membrane depolarization following treatment with the peptides. The mitochondrial membrane depolarization/disruption which leads to apoptosis has been reported as one of the common mechanisms of action for various ACPs. The high affinity of the ACPs for mitochondrial membrane is supposed to be due to its high content of negatively charged lipids such as cardiolipin [30,32,33,36,37]. The peptides which showed high selectivity for cancer cells in the viability tests (IK-13, LK-13, CI-15, and GI-15) were tested for their ability to induce mitochondrial membrane disruption in HCT 116 cells compared to HDF cells.

Fig. 9 shows the images of the HCT 116 and the HDF cells stained with JC-1 mitochondrial probe following treatment with the ACPs. JC-1 is a membrane permeant dye and its accumulation in the mitochondria depends merely on the mitochondrial membrane potential [91,92]. Accumulation of JC-1 in healthy mitochondria results in red fluorescence from the JC-1 aggregates [93,94]. On the other hand, depolarization of the mitochondrial membranes, which is a distinctive feature of the early stages of apoptosis, results in reduced accumulation of JC-1 in the mitochondria manifested by green fluorescence from JC-1 monomers [93,94]. As it could be observed the ACPs damaged the mitochondrial membranes of the HCT 116 cells to a great extent as denoted by higher proportion of green fluorescence compared to red fluorescence. On the contrary, in HDFs the red fluorescence from healthy mitochondria was dominating, indicating less damage to the mitochondrial membrane. This is consistent with lower cellular uptake and lower cytotoxicity of the ACPs in fibroblasts compared to cancer cells as discussed earlier. Hence, the designed ACPs exert their anticancer activity by damaging the mitochondrial membranes which would eventually lead to apoptosis.

4. Conclusion

A series of short cationic amphiphilic α-helical peptides with selective anticancer activity were designed and their structure–activity relationship was studied. The peptides had strong anticancer activity against colorectal cancer cells, cervical cancer cells and colorectal cancer MCTSs with minimal toxicity against normal non-cancerous cells (human dermal fibroblasts). Our designed peptides have modified structures compared to the other anticancer peptides reported in the literature which has resulted in higher selectivity against cancer cells and in some cases even higher potency compared to other peptides reported elsewhere [42,54]. The higher selectivity of the peptides for the cancer cells was attributed to their higher tendency to interact with the negatively charged membrane of the cancer cells compared to the zwitterionic membrane of normal cells. This is consistent with the literature data suggesting cancer cell membrane targeting as the main mechanism of cell selectivity for ACPs [30–34,36,37]. The peptides exerted their cytotoxicity by damaging the mitochondrial membrane which eventually led to apoptosis, which has been reported frequently as one of the main mechanisms of cytotoxicity of many anticancer peptides [30,32,33,36,37]. The anticancer activity of the peptides was directly proportional to their helical content, hydrophobicity and surface activity which is in agreement

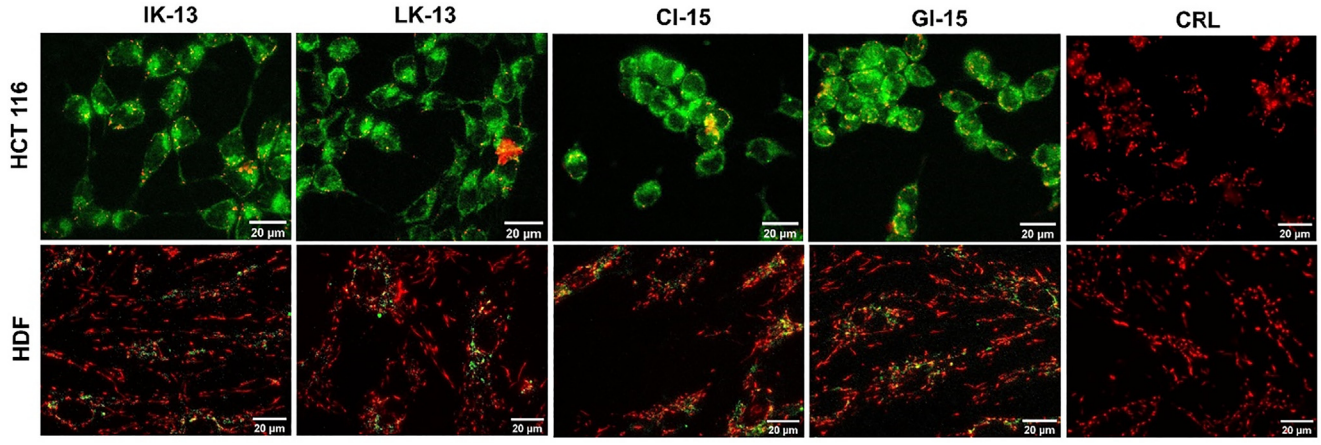

Fig. 9. Mitochondrial membrane depolarization by cationic amphiphilic peptides in HCT 116 (**top panel**) and HDF cells (**bottom panel**) as determined by JC-1 mitochondrial probe. The red fluorescence indicates healthy mitochondria, and the green fluorescence indicates damaged mitochondria in pre-apoptotic cells.

with the results from studies on other types of helical anticancer peptides [39,42,54,70]. The toxicity of peptides in normal cells was mainly affected by the composition of the hydrophilic domain of the peptides with lysine being more favourable than arginine. It was found that addition of isoleucine residues to the C-terminal and a cysteine residue to the *N*-terminal of the peptides significantly enhanced their anticancer activity while maintaining low toxicity in normal cells. These findings provide a basis for rational design of new anticancer peptides with enhanced potency and selectivity through modification of the peptide structure and physicochemical properties. Based on the current findings, it is suggested that in the future attempts for rational design of short α-helical anticancer peptides, the lysine residues would be included in the cationic domain of the peptide instead of arginine residues to avoid the cytotoxic effect of arginine residues on normal cells. Furthermore, presence of a hydrophobic amino acid residue such as isoleucine in the C-terminal of these peptides is more favourable than a hydrophilic amino acid residue such as lysine. Moreover, where stronger helical conformation is desirable, inclusion of cysteine residue in the *N*-terminal of the peptide is recommended. Future work will be aimed at more in depth study of the interaction of the designed anticancer peptides with different cell membranes in order to shed more light on the molecular mechanisms behind specific cell selectivity and also the exact mechanism of membrane translocation of the peptides. Further modification of the peptide sequences to investigate the effect of other types of structural modifications on the biological activity of this class of peptides is another area to be covered by further studies.

CRediT authorship contribution statement

Roja Hadianamrei: Conceptualization, Methodology, Investigation, Validation, Formal analysis, Data curation, Visualization, Writing – original draft, Writing – review & editing. **Mhd Anas Tomeh:** Methodology, Writing – review & editing. **Stephen Brown:** Methodology, Supervision. **Jiqian Wang:** Resources. **Xiubo Zhao:** Conceptualization, Methodology, Visualization, Writing – review & editing, Supervision, Project administration, Funding acquisition.

Declaration of Competing Interest

The authors declare that they have no known competing financial interests or personal relationships that could have appeared to influence the work reported in this paper.

Acknowledgements

We would like to thank EPSRC (EP/N007174/1 and EP/N023579/1), and Royal Society (RG160662 and IE150457) for support. The authors would like to thank Dr Caroline Evans from the Department of Chemical and Biological Engineering, University of Sheffield and Mr Rob Hanson from the Department of Chemistry, University of Sheffield for their technical assistance. RH would like to thank the University of Sheffield for scholarship.

References

[1] M.R. Stratton, P.J. Campbell, P.A. Futreal, The cancer genome, Nature 458 (7239) (2009) 719–724.
[2] F. Martínez-Jiménez, F. Muiños, I. Sentís, J. Deu-Pons, I. Reyes-Salazar, C. Arnedo-Pac, L. Mularoni, O. Pich, J. Bonet, H. Kranas, A. Gonzalez-Perez, N. Lopez-Bigas, A compendium of mutational cancer driver genes, Nat. Rev. Cancer 20 (10) (2020) 555–572.
[3] D.S. Chen, I. Mellman, Elements of cancer immunity and the cancer–immune set point, Nature 541 (7637) (2017) 321–330.
[4] D. Hanahan, Robert A. Weinberg, Hallmarks of Cancer: The Next Generation. Cell 144 (5) (2011) 646-674.
[5] D. Galmarini, C.M. Galmarini, F.C. Galmarini, Cancer chemotherapy: A critical analysis of its 60 years of history, Critical Reviews in Oncology/Hematology 84 (2) (2012) 181–199.
[6] K.D. Jhaveri, H.H. Shah, K. Calderon, E.S. Campenot, J. Radhakrishnan, Glomerular diseases seen with cancer and chemotherapy: a narrative review, Kidney Int. 84 (1) (2013) 34–44.
[7] J. Tamargo, R. Caballero, E. Delpón, Cancer Chemotherapy and Cardiac Arrhythmias: A Review, Drug Saf. 38 (2) (2015) 129–152.
[8] J. Lemieux, E. Maunsell, L. Provencher, Chemotherapy-induced alopecia and effects on quality of life among women with breast cancer: a literature review, Psycho-Oncology 17 (4) (2008) 317–328.
[9] M. Reich, A. Lesur, C. Perdrizet-Chevallier, Depression, quality of life and breast cancer: a review of the literature, Breast Cancer Res. Treat. 110 (1) (2008) 9–17.
[10] J. Pollack, T. Holm, B. Cedermark, D. Altman, B. Holmström, B. Glimelius, A. Mellgren, Late adverse effects of short-course preoperative radiotherapy in rectal cancer, Br. J. Surg. 93 (12) (2006) 1519–1525.
[11] S.L. Kerns, H. Ostrer, B.S. Rosenstein, Radiogenomics: Using Genetics to Identify Cancer Patients at Risk for Development of Adverse Effects Following Radiotherapy, Cancer Discovery 4 (2) (2014) 155.
[12] D. Azria, M. Ozsahin, A. Kramar, S. Peters, D.P. Atencio, N.E.A. Crompton, F. Mornex, A. Pèlegrin, J.-B. Dubois, R.-O. Mirimanoff, B.S. Rosenstein, Single Nucleotide Polymorphisms, Apoptosis, and the Development of Severe Late Adverse Effects After Radiotherapy, Clin. Cancer Res. 14 (19) (2008) 6284.
[13] E. Senkus-Konefka, J. Jassem, Cardiovascular effects of breast cancer radiotherapy, Cancer Treat. Rev. 33 (6) (2007) 578–593.
[14] C. Widakowich, G. de Castro Jr., E. de Azambuja, P. Dinh, A. Awada, Review: Side Effects of Approved Molecular Targeted Therapies in Solid Cancers, The Oncologist 12 (12) (2007) 1443–1455.
[15] M. Stern, R. Herrmann, Overview of monoclonal antibodies in cancer therapy: present and promise, Critical Reviews in Oncology/Hematology 54 (1) (2005) 11–29.
[16] H. Gharwan, H. Groninger, Kinase inhibitors and monoclonal antibodies in oncology: clinical implications, Nat. Rev. Clin. Oncol. 13 (4) (2016) 209–227.
[17] T.T. Hansel, H. Kropshofer, T. Singer, J.A. Mitchell, A.J.T. George, The safety and side effects of monoclonal antibodies, Nat. Rev. Drug Discovery 9 (4) (2010) 325–338.
[18] A.M. Scott, J.D. Wolchok, L.J. Old, Antibody therapy of cancer, Nat. Rev. Cancer 12 (4) (2012) 278–287.
[19] P.A. Mayes, K.W. Hance, A. Hoos, The promise and challenges of immune agonist antibody development in cancer, Nat. Rev. Drug Discovery 17 (7) (2018) 509–527.
[20] A.W. Hahn, D.M. Gill, S.K. Pal, N. Agarwal, The future of immune checkpoint cancer therapy after PD-1 and CTLA-4, Immunotherapy 9 (8) (2017) 681–692.
[21] L. Galluzzi, J. Humeau, A. Buqué, L. Zitvogel, G. Kroemer, Immunostimulation with chemotherapy in the era of immune checkpoint inhibitors, Nat. Rev. Clin. Oncol. 17 (12) (2020) 725–741.
[22] N. Halama, I. Zoernig, A. Berthel, C. Kahlert, F. Klupp, M. Suarez-Carmona, T. Suetterlin, K. Brand, J. Krauss, F. Lasitschka, T. Lerchl, C. Luckner-Minden, A. Ulrich, M. Koch, J. Weitz, M. Schneider, M.W. Buechler, L. Zitvogel, T. Herrmann, A. Benner, C. Kunz, S. Luecke, C. Springfeld, N. Grabe, C.S. Falk, D. Jaeger, Tumoral Immune Cell Exploitation in Colorectal Cancer Metastases Can Be Targeted Effectively by Anti-CCR5 Therapy in Cancer Patients, Cancer Cell 29 (4) (2016) 587–601.
[23] C.H. June, Adoptive T cell therapy for cancer in the clinic, J. Clin. Investig. 117 (6) (2007) 1466–1476.
[24] N.G. Minutolo, E.E. Hollander, D.J. Powell, The Emergence of Universal Immune Receptor T Cell Therapy for Cancer, Front. Oncol. 9 (2019) 176.
[25] L.M. Weiner, R. Surana, S. Wang, Monoclonal antibodies: versatile platforms for cancer immunotherapy, Nat. Rev. Immunol. 10 (5) (2010) 317–327.
[26] L.M. Weiner, M.V. Dhodapkar, S. Ferrone, Monoclonal antibodies for cancer immunotherapy, The Lancet 373 (9668) (2009) 1033–1040.
[27] K. Kingwell, CAR T therapies drive into new terrain, Nat. Rev. Drug Discovery 16 (5) (2017) 301–304.
[28] W. Pichler, P. Campi, Adverse Side Effects to Biological Agents. (2007) 151–165.
[29] J.-C. Marine, S.-J. Dawson, M.A. Dawson, Non-genetic mechanisms of therapeutic resistance in cancer, Nat. Rev. Cancer 20 (12) (2020) 743–756.
[30] B. Deslouches, Y. Peter Di, Antimicrobial peptides with selective antitumor mechanisms: prospect for anticancer applications, Oncotarget 8 (28) (2017) 46635–46651.
[31] M.R. Felício, O.N. Silva, S. Gonçalves, N.C. Santos, O.L. Franco, Peptides with Dual Antimicrobial and Anticancer Activities, Front. Chem. 5 (2017) 5.
[32] D. Gaspar, A.S. Veiga, M.A.R.B. Castanho, From antimicrobial to anticancer peptides. A review, Front. Microbiol. 4 (2013) 294.
[33] S. Riedl, D. Zweytick, K. Lohner, Membrane-active host defense peptides – Challenges and perspectives for the development of novel anticancer drugs, Chem. Phys. Lipids 164 (8) (2011) 766–781.
[34] D.W. Hoskin, A. Ramamoorthy, Studies on anticancer activities of antimicrobial peptides, Biochimica et Biophysica Acta (BBA) - Biomembranes 1778 (2) (2008) 357–375.
[35] D. Wu, Y. Gao, Y. Qi, L. Chen, Y. Ma, Y. Li, Peptide-based cancer therapy: Opportunity and challenge, Cancer Lett. 351 (1) (2014) 13–22.
[36] F. Schweizer, Cationic amphiphilic peptides with cancer-selective toxicity, Eur. J. Pharmacol. 625 (1) (2009) 190–194.

[37] L. Nyström, M. Malmsten, Membrane interactions and cell selectivity of amphiphilic anticancer peptides, Curr. Opin. Colloid Interface Sci. 38 (2018) 1–17.
[38] K. Kurrikoff, D. Aphkhazava, Ü. Langel, The future of peptides in cancer treatment, Curr. Opin. Pharmacol. 47 (2019) 27–32.
[39] H. Gong, J. Zhang, X. Hu, Z. Li, K. Fa, H. Liu, T.A. Waigh, A. McBain, J.R. Lu, Hydrophobic Control of the Bioactivity and Cytotoxicity of de Novo-Designed Antimicrobial Peptides, ACS Appl. Mater. Interfaces 11 (38) (2019) 34609–34620.
[40] C. Chen, C. Yang, Y. Chen, F. Wang, Q. Mu, J. Zhang, Z. Li, F. Pan, H. Xu, J.R. Lu, Surface Physical Activity and Hydrophobicity of Designed Helical Peptide Amphiphiles Control Their Bioactivity and Cell Selectivity, ACS Appl. Mater. Interfaces 8 (40) (2016) 26501–26510.
[41] A.T.Y. Yeung, S.L. Gellatly, R.E.W. Hancock, Multifunctional cationic host defence peptides and their clinical applications, Cell. Mol. Life Sci. 68 (13) (2011) 2161.
[42] C. Chen, Y. Chen, C. Yang, P. Zeng, H. Xu, F. Pan, J.R. Lu, High Selective Performance of Designed Antibacterial and Anticancer Peptide Amphiphiles, ACS Appl. Mater. Interfaces 7 (31) (2015) 17346–17355.
[43] C. Chen, J. Hu, S. Zhang, P. Zhou, X. Zhao, H. Xu, X. Zhao, M. Yaseen, J.R. Lu, Molecular mechanisms of antibacterial and antitumor actions of designed surfactant-like peptides, Biomaterials 33 (2) (2012) 592–603.
[44] Z.Y. Ong, N. Wiradharma, Y.Y. Yang, Strategies employed in the design and optimization of synthetic antimicrobial peptide amphiphiles with enhanced therapeutic potentials, Adv. Drug Deliv. Rev. 78 (2014) 28–45.
[45] F. Grisoni, C.S. Neuhaus, M. Hishinuma, G. Gabernet, J.A. Hiss, M. Kotera, G. Schneider, De novo design of anticancer peptides by ensemble artificial neural networks, J. Mol. Model. 25 (5) (2019) 112.
[46] Y.-C. Lin, Y.F. Lim, E. Russo, P. Schneider, L. Bolliger, A. Edenharter, K.-H. Altmann, C. Halin, J.A. Hiss, G. Schneider, Multidimensional Design of Anticancer Peptides, Angew. Chem. Int. Ed. 54 (35) (2015) 10370–10374.
[47] A. Tyagi, P. Kapoor, R. Kumar, K. Chaudhary, A. Gautam, G.P.S. Raghava, In Silico Models for Designing and Discovering Novel Anticancer Peptides, Sci. Rep. 3 (1) (2013) 2984.
[48] G. Gabernet, D. Gautschi, A.T. Müller, C.S. Neuhaus, L. Armbrecht, P.S. Dittrich, J.A. Hiss, G. Schneider, In silico design and optimization of selective membranolytic anticancer peptides, Sci. Rep. 9 (1) (2019) 11282.
[49] I. Zelezetsky, A. Tossi, Alpha-helical antimicrobial peptides—Using a sequence template to guide structure–activity relationship studies, Biochimica et Biophysica Acta (BBA) - Biomembranes 1758 (9) (2006) 1436–1449.
[50] Y. Liscano, J. Oñate-Garzón, J.P. Delgado, Peptides with Dual Antimicrobial-Anticancer Activity: Strategies to Overcome Peptide Limitations and Rational Design of Anticancer Peptides, Molecules (Basel, Switzerland) 25 (18) (2020) 4245.
[51] Z.Y. Ong, J. Cheng, Y. Huang, K. Xu, Z. Ji, W. Fan, Y.Y. Yang, Effect of stereochemistry, chain length and sequence pattern on antimicrobial properties of short synthetic β-sheet forming peptide amphiphiles, Biomaterials 35 (4) (2014) 1315–1325.
[52] S.R. Dennison, F. Harris, T. Bhatt, J. Singh, D.A. Phoenix, The effect of C-terminal amidation on the efficacy and selectivity of antimicrobial and anticancer peptides, Mol. Cell. Biochem. 332 (1) (2009) 43.
[53] E. Crusca Jr, A.A. Rezende, R. Marchetto, M.J.S. Mendes-Giannini, W. Fontes, M. S. Castro, E.M. Cilli, Influence of N-terminus modifications on the biological activity, membrane interaction, and secondary structure of the antimicrobial peptide hylin-a1, Pept. Sci. 96 (1) (2011) 41–48.
[54] C. Chen, J. Hu, P. Zeng, F. Pan, M. Yaseen, H. Xu, J.R. Lu, Molecular mechanisms of anticancer action and cell selectivity of short α-helical peptides, Biomaterials 35 (5) (2014) 1552–1561.
[55] D. Eisenberg, R.M. Weiss, T.C. Terwilliger, The helical hydrophobic moment: a measure of the amphiphilicity of a helix, Nature 299 (5881) (1982) 371–374.
[56] D. Eisenberg, E. Schwarz, M. Komaromy, R. Wall, Analysis of membrane and surface protein sequences with the hydrophobic moment plot, J. Mol. Biol. 179 (1) (1984) 125–142.
[57] V. Pliška, M. Schmidt, J.-L. Fauchère, Partition coefficients of amino acids and hydrophobic parameters π of their side-chains as measured by thin-layer chromatography, J. Chromatogr. A 216 (1981) 79–92.
[58] J.-L. Fauchère, V. Pliska, Hydrophobic parameters Π of amino-acid side chains from the partitioning of N-acetyl-amino-acid amides, Eur. J. Med. Chem. 18 (4) (1983) 7.
[59] N. Wiradharma, U. Khoe, C.A.E. Hauser, S.V. Seow, S. Zhang, Y.-Y. Yang, Synthetic cationic amphiphilic α-helical peptides as antimicrobial agents, Biomaterials 32 (8) (2011) 2204–2212.
[60] Z.Y. Ong, S.J. Gao, Y.Y. Yang, Short Synthetic β-Sheet Forming Peptide Amphiphiles as Broad Spectrum Antimicrobials with Antibiofilm and Endotoxin Neutralizing Capabilities, Adv. Funct. Mater. 23 (29) (2013) 3682–3692.
[61] J.S. Khara, F.K. Lim, Y. Wang, X.-Y. Ke, Z.X. Voo, Y.Y. Yang, R. Lakshminarayanan, P.L.R. Ee, Designing α-helical peptides with enhanced synergism and selectivity against Mycobacterium smegmatis: Discerning the role of hydrophobicity and helicity, Acta Biomater. 28 (2015) 99–108.
[62] A. Hollmann, M. Martínez, M.E. Noguera, M.T. Augusto, A. Disalvo, N.C. Santos, L. Semorile, P.C. Maffía, Role of amphipathicity and hydrophobicity in the balance between hemolysis and peptide–membrane interactions of three related antimicrobial peptides, Colloids Surf., B 141 (2016) 528–536.
[63] C.-S.C. Wu, K. Ikeda, J.T. Yang, Ordered conformation of polypeptides and proteins in acidic dodecyl sulfate solution, Biochemistry 20 (3) (1981) 566–570.
[64] Y.-H. Chen, J.T. Yang, H.M. Martinez, Determination of the secondary structures of proteins by circular dichroism and optical rotatory dispersion, Biochemistry 11 (22) (1972) 4120–4131.
[65] R. Maget-Dana, The monolayer technique: a potent tool for studying the interfacial properties of antimicrobial and membrane-lytic peptides and their interactions with lipid membranes, Biochimica et Biophysica Acta (BBA) - Biomembranes 1462 (1) (1999) 109–140.
[66] D. Ciumac, R.A. Campbell, L.A. Clifton, H. Xu, G. Fragneto, J.R. Lu, Influence of Acyl Chain Saturation on the Membrane-Binding Activity of a Short Antimicrobial Peptide, ACS Omega 2 (11) (2017) 7482–7492.
[67] T. Kiyota, S. Lee, G. Sugihara, Design and Synthesis of Amphiphilic α-Helical Model Peptides with Systematically Varied Hydrophobic−Hydrophilic Balance and Their Interaction with Lipid- and Bio-Membranes, Biochemistry 35 (40) (1996) 13196–13204.
[68] D.L. Steer, P.E. Thompson, S.E. Blondelle, R.A. Houghten, M.-I. Aguilar, Comparison of the binding of α-helical and β-sheet peptides to a hydrophobic surface, The Journal of Peptide Research 51 (6) (1998) 401–412.
[69] Y. Chen, M.T. Guarnieri, A.I. Vasil, M.L. Vasil, C.T. Mant, R.S. Hodges, Role of peptide hydrophobicity in the mechanism of action of alpha-helical antimicrobial peptides, Antimicrob. Agents Chemother. 51 (4) (2007) 1398–1406.
[70] S. Kim, S.S. Kim, B.J. Lee, Correlation between the activities of α-helical antimicrobial peptides and hydrophobicities represented as RP HPLC retention times, Peptides 26 (11) (2005) 2050–2056.
[71] S.E. Blondelle, J.M. Ostresh, R.A. Houghten, E. Pérez-Payá, Induced conformational states of amphipathic peptides in aqueous/lipid environments, Biophys. J . 68 (1) (1995) 351–359.
[72] M. Majerowicz, A.J. Waring, S. Wen, F. Bringezu, Interaction of the Antimicrobial Peptide Dicynthaurin with Membrane Phospholipids at the Air−Liquid Interface, J. Phys. Chem. B 111 (14) (2007) 3813–3821.
[73] E. Eiríksdóttir, K. Konate, Ü. Langel, G. Divita, S. Deshayes, Secondary structure of cell-penetrating peptides controls membrane interaction and insertion, Biochimica et Biophysica Acta (BBA) - Biomembranes 1798 (6) (2010) 1119–1128.
[74] J. Hu, C. Chen, S. Zhang, X. Zhao, H. Xu, X. Zhao, J.R. Lu, Designed Antimicrobial and Antitumor Peptides with High Selectivity, Biomacromolecules 12 (11) (2011) 3839–3843.
[75] M. Schiffer, A.B. Edmundson, Use of helical wheels to represent the structures of proteins and to identify segments with helical potential, Biophys J 7 (2) (1967) 121–135.
[76] D.V. LaBarbera, B.G. Reid, B.H. Yoo, The multicellular tumor spheroid model for high-throughput cancer drug discovery, Expert Opin. Drug Discov. 7 (9) (2012) 819–830.
[77] T. Rodrigues, B. Kundu, J. Silva-Correia, S.C. Kundu, J.M. Oliveira, R.L. Reis, V.M. Correlo, Emerging tumor spheroids technologies for 3D in vitro cancer modeling, Pharmacol. Ther. 184 (2018) 201–211.
[78] E.-T. Verjans, J. Doijen, W. Luyten, B. Landuyt, L. Schoofs, Three-dimensional cell culture models for anticancer drug screening: Worth the effort?, J Cell. Physiol. 233 (4) (2018) 2993–3003.
[79] M. Zanoni, S. Pignatta, C. Arienti, M. Bonafè, A. Tesei, Anticancer drug discovery using multicellular tumor spheroid models, Expert Opin. Drug Discov. 14 (3) (2019) 289–301.
[80] S. Grissenberger, S. Riedl, B. Rinner, R. Leber, D. Zweytick, Design of human lactoferricin derived antitumor peptides-activity and specificity against malignant melanoma in 2D and 3D model studies, Biochimica et Biophysica Acta (BBA) - Biomembranes 1862 (8) (2020) 183264.
[81] N. Dhiman, N. Shagaghi, M. Bhave, H. Sumer, P. Kingshott, S.N. Rath, Selective Cytotoxicity of a Novel Trp-Rich Peptide against Lung Tumor Spheroids Encapsulated inside a 3D Microfluidic Device, Adv. Biosyst. 4 (4) (2020) 1900285.
[82] F.-H. Liu, C.-Y. Hou, D. Zhang, W.-J. Zhao, Y. Cong, Z.-Y. Duan, Z.-Y. Qiao, H. Wang, Enzyme-sensitive cytotoxic peptide–dendrimer conjugates enhance cell apoptosis and deep tumor penetration, Biomater. Sci. 6 (3) (2018) 604–613.
[83] C. Hu, X. Chen, Y. Huang, Y. Chen, Co-administration of iRGD with peptide HPRP-A1 to improve anticancer activity and membrane penetrability, Sci. Rep. 8 (1) (2018) 2274.
[84] H.-R. Jia, Y.-X. Zhu, K.-F. Xu, F.-G. Wu, Turning Toxicants into Safe Therapeutic Drugs: Cytolytic Peptide−Photosensitizer Assemblies for Optimized In Vivo Delivery of Melittin, Adv. Healthcare Mater. 7 (16) (2018) 1800380.
[85] R. Maget-Dana, A. Brack, D. Lelievre, Amphiphilic peptides as models for protein-membrane interactions: interfacial behaviour of sequential Lys- and Leu-based peptides and their penetration into lipid monolayers, Supramol. Sci. 4 (3) (1997) 365–368.
[86] D. Ciumac, H. Gong, X. Hu, J.R. Lu, Membrane targeting cationic antimicrobial peptides, J. Colloid Interface Sci. 537 (2019) 163–185.
[87] D. Ciumac, R.A. Campbell, H. Xu, L.A. Clifton, A.V. Hughes, J.R.P. Webster, J.R. Lu, Implications of lipid monolayer charge characteristics on their selective interactions with a short antimicrobial peptide, Colloids Surf., B 150 (2017) 308–316.
[88] A. Hädicke, A. Blume, Binding of the Cationic Peptide (KL)4K to Lipid Monolayers at the Air-Water Interface: Effect of Lipid Headgroup Charge,

Acyl Chain Length, and Acyl Chain Saturation, J. Phys. Chem. B 120 (16) (2016) 3880–3887.
[89] A. Schmidtchen, M. Pasupuleti, M. Malmsten, Effect of hydrophobic modifications in antimicrobial peptides, Adv. Colloid Interface Sci. 205 (2014) 265–274.
[90] L. Ringstad, A. Schmidtchen, M. Malmsten, Effect of Peptide Length on the Interaction between Consensus Peptides and DOPC/DOPA Bilayers, Langmuir 22 (11) (2006) 5042–5050.
[91] S.T. Smiley, M. Reers, C. Mottola-Hartshorn, M. Lin, A. Chen, T.W. Smith, G.D. Steele, L.B. Chen, Intracellular heterogeneity in mitochondrial membrane potentials revealed by a J-aggregate-forming lipophilic cation JC-1. Proceedings of the National Academy of Sciences 88 (9) (1991) 3671.
[92] M. Reers, T.W. Smith, L.B. Chen, J-aggregate formation of a carbocyanine as a quantitative fluorescent indicator of membrane potential, Biochemistry 30 (18) (1991) 4480–4486.
[93] M. Mancini, B.O. Anderson, E. Caldwell, M. Sedghinasab, P.B. Paty, D.M. Hockenbery, Mitochondrial Proliferation and Paradoxical Membrane Depolarization during Terminal Differentiation and Apoptosis in a Human Colon Carcinoma Cell Line, J. Cell Biol. 138 (2) (1997) 449–469.
[94] G.V. Kulkarni, W. Lee, A. Seth, C.A.G. McCulloch, Role of Mitochondrial Membrane Potential in Concanavalin A-Induced Apoptosis in Human Fibroblasts, Exp. Cell Res. 245 (1) (1998) 170–178.